Biochimica et Biophysica Acta 1818 (2012) 2354–2361

Contents lists available at SciVerse ScienceDirect

Biochimica et Biophysica Acta

journal homepage: www.elsevier.com/locate/bbamem

Gly_6 of kalata B1 is critical for the selective binding to phosphatidylethanolamine membranes

Kristopher Hall [a], Tzong-Hsien Lee [a], Norelle L. Daly [b], David J. Craik [b], Marie-Isabel Aguilar [a,*]

[a] Department of Biochemistry & Molecular Biology, Monash University, Clayton Vic 3800, Australia
[b] Institute for Molecular Bioscience, The University of Queensland, Brisbane Qld 4072, Australia

ARTICLE INFO

Article history:
Received 21 November 2011
Received in revised form 29 March 2012
Accepted 10 April 2012
Available online 17 April 2012

Keywords:
SPR
AFM
Peptide–lipid interaction
Antimicrobial peptide
Cyclotide
Phospholipid membrane

ABSTRACT

The membrane interaction of the cyclotide kalata B1, an all-D-analogue and a single alanine substituted analogue (G6A), was studied by surface plasmon resonance (SPR) and atomic force microscopy (AFM). Kalata B1 showed a strong binding selectivity for dimyristoyl-phosphatidylethanolamine (DMPE) compared to dimyristoyl-phoshatidylcholine (DMPC)-containing lipids. However, when the interaction was visualized by AFM the peptide interacted with DMPC and DMPE in a similar manner. There was no apparent change in membrane morphology with either lipid, suggesting that kalata B1 does not act via a carpet-like disruption mechanism. The D-analogue showed similar binding by SPR and the same strong selectivity for DMPE, indicating that the membrane-interaction and lipid selectivity are not stereo-specific. SPR studies of the G6A analogue revealed that it interacted in a similar way to kalata B1 on the DMPC containing lipids, but showed no increased response on the DMPE containing lipids observed for kalata B1 and D-kalata B1. These results indicate that the Gly6 residue directly influences membrane binding as it is located near a putative membrane interacting hydrophobic patch. Overall, the data suggest that very small changes in amino acid composition (with no change in conformation) can influence specific self-association in combination with membrane binding and mediate the activity of kalata B1.

1. Introduction

Cyclotides [1,2] are a family of plant-derived mini-proteins that comprise around 30 amino acids and are characterised by their distinct combination of a cyclized backbone (their C and N termini are linked together via a peptide bond) and six highly conserved cystine residues that form a knotted arrangement of cross-linking disulfide bonds. The combination of these two structural characteristics makes cyclotides resistant to enzymatic breakdown and imparts a variety of properties that are attractive for agricultural applications [3] and as molecular scaffolds for pharmaceutical design [4].

The first member of this family to be identified was kalata B1 [5], which was discovered through anecdotal reports of its medicinal use by African women in a tea made from the plant *Oldenlandia affinis* (Rubiaceae) to accelerate childbirth [6]. Many cyclotides have now been discovered in species of the Rubiaceae (coffee) [7,8] and Violaceae (violet) [1,9,10] plant families, with over 200 sequences reported to date (www.CyBase.org.au). In artificial feeding trials a number of cyclotides cause a potent inhibition of growth and development of the cotton bollworm and budworm so their primary natural function appears to be as a host defence in plants against insect pests [3,11]. In addition to their insecticidal and uterotonic activity, anti-tumour [12], anti-HIV [7,13], haemolytic [9] and antibacterial [14] activities have been reported. Kalata B1 has also been reported to have cytolytic activity against a variety of microbes [14] and is weakly haemolytic, with 50% red blood cell hemolysis at 1.5 mM [14].

The mechanism by which cyclotides exert their multiple effects is currently unknown. There is no evidence that they are receptor mediated and studies have shown that they interact with membranes [15–17], possibly acting by forming self-associating multimeric species [18]. Three dimensional structures have highlighted the existence of a surface exposed patch of hydrophobic residues that might be involved in membrane binding [19]. The circular sequence, three dimensional structure, and knotted arrangement of the three conserved disulfide bonds of kalata B1 is shown in Fig. 1. As mentioned previously, it is this cyclic backbone and the cystine knot that give cyclotides their resistance to thermal, chemical and enzymatic breakdown compared to linear peptides of similar size [20]. It is these properties that make

Abbreviations: AMP, antimicrobial peptides; CD, circular dichroism; CHAPS, 3-[(cholamidopropyl)dimethyl-ammonio]-1-propane sulfonate; DMPC, 1,2-dimyristoyl-sn-glycero-3-phosphocholine; DMPG, 1,2-dimyristoyl-sn-glycero-3-[phospho-rac-(1-glycerol)]; DMPE, 1,2-dimyristoyl-*sn*-Glycero-3-phosphoethanolamine; MIC, minimum inhibitory concentration; MLV, multilamellar vesicle; PC, phosphatidylcholine; PG, phospho-rac-(1-glycerol); SPR, surface plasmon resonance; AFM, atomic force microscopy

* Corresponding author. Tel.: +61 3 9905 3723; fax: +61 3 9902 9500.
E-mail address: mibel.aguilar@monash.edu (M.-I. Aguilar).

0005-2736/$ – see front matter © 2012 Elsevier B.V. All rights reserved.
doi:10.1016/j.bbamem.2012.04.007

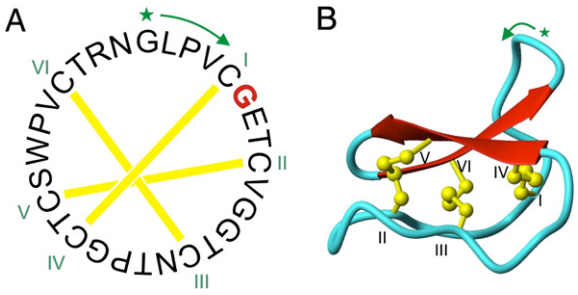

Fig. 1. A) Circular sequence of kalata B1 showing the disulfide bonds with interconnecting yellow lines between paired cysteine residues (labelled in Roman numerals). The green star denotes residue 1 and the green arrow indicates the direction of amino acid residue numbering; B) three dimensional NMR structure of kalata B1 in ribbon format showing β-strands as red arrows and the disulfide bonds shown in ball and stick format [23].

the peptide attractive as a protein scaffold for stabilizing bioactive peptide epitopes to create novel peptide drugs [2,4,21].

The binding of kalata peptides to model membranes was first studied using SPR for two naturally occurring cyclotides from *O. affinis* [15]. The study revealed that dramatic changes in membrane binding properties were observed with different lipid mixtures, and both kalata B1 and kalata B6 showed binding selectivity toward DMPE lipid mixtures. A later study demonstrated that kalata B1 induces leakage in vesicles and pores in model membranes as measured by electrophysiology techniques [17]. Very recently, we reported that an all D-kalata B1 (comprised of all D-amino acids instead of the naturally occurring L-amino acids) bound to model membranes with only slightly decreased affinity to the natural L-peptide [22]. In the current investigation, the binding of L- and D-kalata B1 was further studied together with an Ala mutant identified recently to be inactive in insecticidal assays [23]. In an alanine scan of kalata B1 the analogue in which Gly was replaced by Ala at position 6 (G6A) showed a dramatic decrease in insecticidal activity compared to kalata B1 [23]. In order to explore the role of membrane binding in the large differences in haemolytic and insecticidal activity, the binding of kalata B1, D-kalata B1 and the G6A analogue to model membranes was studied. The results were correlated with secondary structure and the effects of kalata B1 on membrane morphology.

2. Materials and methods

2.1. Chemicals and reagents

Sodium phosphate dibasic/monobasic, (3-cholamidopropyl)-dimethylammonio]-1-propanesulfonate) (CHAPS), 1,2-dimyristoyl-*sn*-glycero-3-phosphocholine (DMPC), 1,2-dimyristoyl-*sn*-glycero-3-[phospho-*rac*-(1-glycerol)] (sodium Salt) (DMPG), 1,2-dimyristoyl-*sn*-glycero-3-phosphoethanolamine (DMPE), and cholesterol, were purchased from Sigma (St Louis, MO, USA). Sodium Chloride was purchased from Spectrum Chemical (Gardena, CA, USA). Choloroform and methanol were purchased from Merck (Vic, Australia).

Table 1
Sequence and masses of kalata B1 and the G6A analogue.

Peptide	Sequence	M_r
Kalata B1	GLPVC**G**ETCVGGTCNTPGCTCSWPVCTRN (cyclic)	2892
G6A	GLPVC**A**ETCVGGTCNTPGCTCSWPVCTRN (cyclic)	2906

Water was quartz-distilled and deionised in a Milli-Q system (Millipore, Bedford, MA, USA). Kalata B1, D-kalata B1 and G6A were synthesised by solid phase peptide synthesis, purified by reversed phase high performance liquid chromatography and the correct mass was determined by electrospray mass spectrometry as previously described [18,22,23] (Table 1).

2.2. Liposome preparation

DMPC and cholesterol were dissolved in chloroform, DMPG was dissolved in a mixture of chloroform/methanol (3:1 v/v) and DMPE was dissolved in a mixture of chloroform/methanol (1:1 v/v) to create individual stock solutions. These stock solutions were then aliquoted into test tubes in the desired molar ratios: DMPC, DMPC/DMPG (4:1 v/v), DMPC/DMPG/cholesterol (16:4:5 v/v), DMPE, DMPE/DMPG (4:1 v/v). The solvent was evaporated under a gentle stream of N_2 and vacuum desiccated overnight. For circular dichroism experiments, lipids were resuspended in 20 mM phosphate buffer with 150 mM NaCl (pH 7.4) with vortexing to a concentration of 1.36 mM. The resultant lipid dispersion was then sonicated with a bath type sonicator until clear. For surface plasmon resonance experiments, lipids were resuspended into buffer with vortexing to a concentration of 0.5–1 mM. The lipid dispersion was then sonicated in a bath type sonicator until nearly clear. Small unilamellar vesicles (SUV; 50 nm) were created via extruding the sonicated mixture through a 50 nm polycarbonate membrane (Avestin). For AFM experiments, lipids were resuspended in buffer to a concentration of 0.1–0.5 mM, vortexed and sonicated briefly before use.

2.3. Circular dichroism (CD)

CD measurements were carried out on a Jasco J-810 Circular Dichroism Spectropolariser (Jasco, Tokyo Japan). Using quartz cells of a 1 mm path length, scans between wavelengths of 190 and 260 nm were done with a scan speed of 20 nm/min and a bandwidth of 1.0 nm. The resolution was 0.1 nm with a 1 s response time, 5 scan accumulations. The quartz cell temperature was controlled with a peltier temperature controller at 25 °C. The CD instrument was calibrated with (+)-10-camphorsulphonic acid. The different lipid liposomes were prepared as above. The concentration of these lipids was 1.36 mM. Once the lipid solution was ready, peptide was then added to a peptide lipid ratio of approximately 1:100. This was then sonicated briefly just before measurements. The concentration of peptide was determined by absorbance at 280 nm ($\varepsilon 100 = 5875\ M^{-1}\ cm^{-1}$). The same peptide concentration was used for samples with peptide in the buffer solution alone. The CD spectra were measured for the peptides in the phosphate buffer solution and in the presence of the different lipid liposomes. The CD signal resulting from the solvent alone was subtracted from the spectrum of each peptide solution. The final spectra obtained for each was the average of the 5 scans accumulated. Spectra were smoothed using the Jasco Fast Fourier transform algorithm and baseline corrected.

2.4. Surface plasmon resonance (SPR)

SPR experiments were carried out with a Biacore 3000 analytical system with an L1 sensor chip (Biacore, Uppsala, Sweden). The system was cleaned using the 'Desorb and Sanitize' protocol with a maintenance chip and then allowed to run overnight with water. The L1 chip was docked and first washed with an injection of 5 μl of 20 mM CHAPS at a flow rate of 5 μl/min to clean the chip surface. SUVs in immobilization buffer (20 mM phosphate buffer 150 mM NaCl pH 7.4) were then immediately applied to the chip surface with injections of 80 μl at a low flow rate of 2 μl/min. To remove any multi-lamellar structures from the lipid surface and to stabilize the baseline, 30 μl of

10 mM NaOH was injected at 50 µl/min. All solutions were freshly prepared, degassed and filtered through a 0.2 µm filter.

Peptide solutions were prepared by dissolving each of peptide in the running buffer (20 mM phosphate buffer 150 mM NaCl pH 7.4), creating 5 serial dilutions of 10 µM to 50 µM. 100 µl of these solutions was injected at a flow rate of 30 µl/min having a total injection time of 200 s. On completion of injection, buffer flow continued to allow a dissociation time of at least 600 s. Buffer-only blank injections were also made to ensure minimal bulk effects. All binding experiments were carried out at 25 °C. Kinetic analysis of the sensorgrams, collected from peptide injections at different concentrations over each different lipid surface, was performed using the Langmuir, the parallel and the two state curve fitting models as described in previous [15,24–26] investigations for other peptide–membrane interactions

2.5. Atomic force microscopy (AFM)

AFM experiments were performed on a Multimode/Nanoscope IV AFM (Digital Instruments, CA, USA) using a vertical engage 'E' scanner. Images were performed in buffer via taping mode with NSC-36 'B' silicon cantilevers (Micromasch, Tallinn, Estonia) with a nominal force constant of 1.75 N/m. 20 µl of freshly prepared lipid solution was deposited onto freshly cleaved mica that had been glued to a metal disc, this was then heated to 40 °C to assist fusion of vesicles on the surface. After 30 minutes incubation, the sample surface was rinsed 3 times with buffer. The sample was then imaged in buffer using the liquid cell. Once a lipid layer was observed, 15 µl of 10 µM peptide was injected and the resultant images were observed. Topographic, phase and amplitude images at a resolution of 512×512 were simultaneously obtained using scan frequencies between 0.5 and 1.5 Hz with typical scan sizes of 5 µm×5 µm, 2 µm×2 µm, 1 µm×1 µm or 500 nm×500 nm. Minimal force was used to reduce the tip effect on the sample. Images were processed with plane fitting and some flattening using WSxM 4.0 software [27].

3. Results

3.1. Secondary structure analysis

The secondary structure of kalata B1 was investigated by circular dichroism in buffer and in the presence of DMPC, DMPC/DMPG (4:1), DMPC/DMPG/cholesterol (16:4:5), and DMPE and DMPE/DMPG (4:1) liposomes. Fig. 2 shows the CD spectra of kalata B1 in buffer and in the presence of the different liposomes. In each case, kalata B1 showed a mixture of secondary structures which is consistent with previously reported CD studies [20,22]. Solubility problems in DMPE precluded consistent spectra to be obtained for this lipid (data not included). The main feature of both sets of published data at wavelengths > 200 nm is the broad minimum centred at approximately 223 nm, which is very similar to the spectra we present in Fig. 2. The difference between each lipid solution occurs below 200 nm which we have found can be due to light scattering of lipid mixtures. The peptide is predominately β-sheet-like in buffer and in the presence of each of the different liposomes and the different lipid mixtures had little influence on the structure.

3.2. Membrane binding properties

The real-time membrane binding interaction of kalata B1, D-kalata B1 and G6A was investigated by SPR on DMPC, DMPC/DMPG (4:1), DMPC/DMPG/cholesterol (16:4:5), and DMPE and DMPE/DMPG (4:1) lipid layers. Five different concentration curves were obtained with 10, 20, 30, 40 and 50 µM to yield a series of sensorgrams shown in Fig. 3.

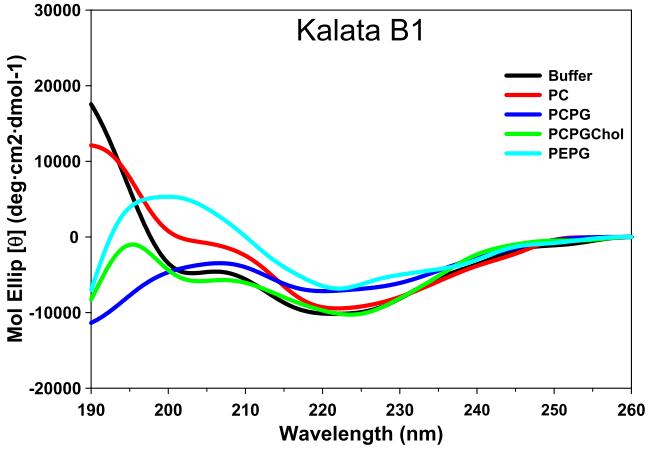

Fig. 2. The CD spectra of kalata B1 in buffer and with different liposomes. 13.6 µM peptide was used with a peptide to lipid ratio of 1:100.

3.2.1. Kalata B1

Fig. 3 shows typical sensorgrams for the binding of kalata B1 to the different membrane layers. Kalata B1 showed fast binding on DMPC in the first initial seconds of the injection, after which the association rate slowed in a second phase of the association. There was also a linear concentration-dependent increase in response. The highest concentration (50 µM) reached a maximum response of 300 RU. The dissociation was very fast, with most of the peptide dissociating from the surface in the first few seconds after completion of the injection. A small amount of peptide remained on the surface at 600 s.

Kalata B1 had a similar response on DMPC/DMPG and DMPC/DMPG/cholesterol, but the response was lower with a maximum response of 200 and 150 RU respectively for the highest concentrations tested. The overall shape of the curves was similar, with the same two-phase association and rapid dissociation with only a small amount of peptide remaining on the DMPC/DMPG membrane layer and no peptide remaining on the DMPC/DMPG/cholesterol layer.

In contrast, kalata B1 had a very different response on lipid layers containing DMPE compared to lipid layers containing DMPC. There was a much greater response on DMPE, with the highest concentration (50 µM) reaching 2400 RU and on DMPE/DMPG reaching a slightly lower maximum response of 1900 RU at 50 µM peptide. The shape of the curves was also quite different compared to those on the DMPC containing lipid layers. Although the peptide reached a greater maximum response, the rate of association was slower. Initially, the 10 µM concentration bound quickly but reached equilibrium by the end of the injection. As the concentration increased, the rate of association changed with the higher concentrations taking longer to reach equilibrium, with the top concentrations failing to reach equilibrium. The dissociation was also slow for the peptide on the lipid layers containing DMPE, with a small amount of peptide remaining on the surface after 600 s.

3.2.2. All D-kalata B1

Fig. 3 also shows typical sensorgrams for the binding of the all D-kalata B1 peptide on the five different lipid layers. D-Kalata B1 showed similar binding to the all L-isomer on DMPC. There was a fast initial interaction then a 2nd slower phase of association. This 2nd phase of the association was a little faster than that of kalata B1 on this lipid layer. There was also a linear concentration dependent increase in response and the highest concentration (50 µM) bound to 350 RU before a rapid dissociation on completion of the injection. The curves reached dissociation equilibrium quickly with approximately 120 RU left on the surface after 600 s.

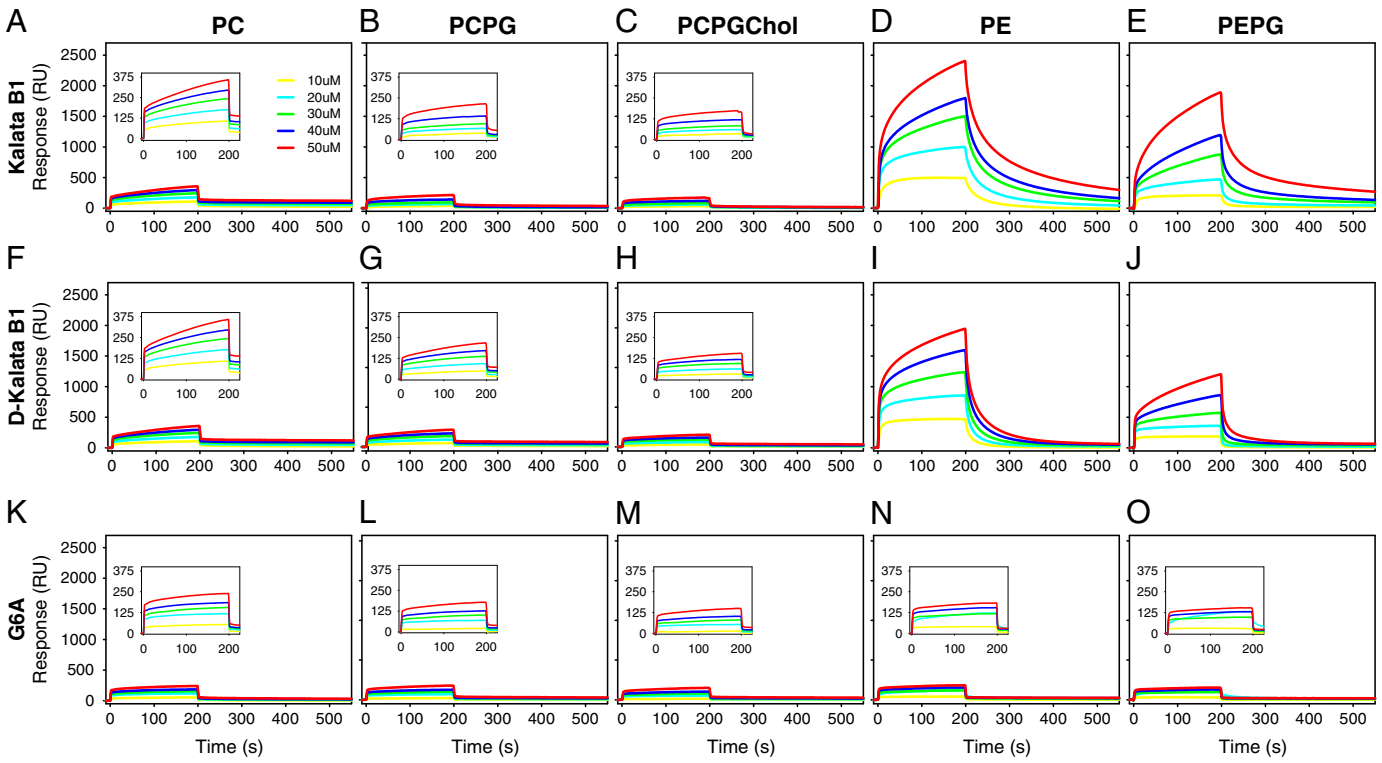

Fig. 3. Typical SPR sensorgrams of kalata B1 (A–E), D-kalata B1 (F–J) and G6A (K–O) on the different lipid bilayer mixtures, DMPC (A, F, K); DMPC/DMPG (4:1) (B, G, L); DMPC/DMPG/cholesterol (16:4:5) (C, H, M); DMPE (D, I, N); DMPE/DMPG (4:1) (E, J, O). Inset boxes are magnified scale. Sensorgrams were obtained at 5 different peptide concentrations from 10 to 50 μM. Injections were 200 s (t = 0–200 s) at 30 μl/min and then the peptide was allowed to dissociate for a further 400 s (t = 200–600 s) as buffer continued to flow through the system.

D-Kalata B1 showed similar results on DMPC/DMPG but there was a slightly lower response. The highest concentration bound up to 200 RU with a similar two phase association before a rapid dissociation again with very little remaining on the surface at 600 s. The results of the peptide on the DMPC/DMPG/cholesterol layer are almost identical to that on the DMPC/DMPG layer but the response is slightly lower. The highest concentration reached a maximum of 150 RU.

D-Kalata B1 showed a greater response on the lipids containing DMPE, similar to L-Kalata B1 than the DMPC containing lipids. The peptide bound quickly in the first few seconds but then showed a slower 2nd phase of association comparable to the slow phase on the DMPC lipids. The dissociation was also slower, and the peptide dissociated completely from the surface. The results were similar again on DMPE/DMPG with a similar shaped association and dissociation to the sensorgrams for DMPE, but the response was lower with the highest concentration binding up to 1250 RU.

3.2.3. Alanine substituted G6A

Fig. 3 shows typical sensorgrams for the alanine substituted G6A analogue on the different model membrane layers. G6A showed a similar binding profile as the other two peptides on DMPC. There was fast initial binding in the first few seconds which then slowed and levelled out to reach a response of 230 RU at 50 μM concentration. The dissociation was almost instantaneous with only a small amount of peptide remaining on the surface in only a few seconds after the end of injection.

The response was similar on DMPC/DMPG and DMPC/DMPG/cholesterol layers with similar shaped curves. However, the response was slightly lower with the 50 μM concentration reaching a maximum of 170 and 130 RU respectively. The same fast association and dissociation were also evident.

However, G6A showed a completely different interaction with the membranes containing DMPE. In contrast to kalata B1 and the all-D analogue which showed a large increase in response on DMPE compared to the lipids containing DMPC, G6A did not show this strong binding. The peptide interacted in a similar way with DMPE as with the DMPC membranes with a fast initial binding and then a slower association phase up to a maximum response of 200 RU on DMPE and 150 RU on DMPE/DMPG with the 50 μM concentration. G6A again showed a fast dissociation with no peptide remaining on the surface after only a few seconds of dissociation.

3.2.4. Quantitative analysis of sensorgrams

Kinetic analysis of the sensorgrams shown in Fig. 3 was performed via curve fitting to the different models detailed previously [28–30]. Curve fitting using the 1:1 Langmuir model, the two state model and the heterogeneous model yielded moderate quality fits for DMPC, DMPC/DMPG and DMPC/DMG/cholesterol. However, significantly poorer fits were observed for DMPE and DMPE/DMPG (results not shown) for which the chi^2 values were very high (>2000 RU), which is a reflection of the changing shape of the sensorgrams with increasing peptide concentration. Overall, it was not possible to make quantitative conclusions about the relative changes in affinity based on this analysis across the different membrane systems. This clearly demonstrates the complexity of the interaction, which may involve different kinetic steps of surface binding, insertion and self-association which preclude reliable determination of overall rate and affinity constants.

In order to allow a semi-quantitative comparison between the two peptides, the RU at the end of the association phase (at 200 s) was plotted against peptide concentration [28] and shown in Fig. 4 for (a) L-kalata, (b) D-kalata and (c) G6A. While these plots illustrate a shallow, linear dependence on concentration for the DMPC-containing bilayers, there was a strong concentration dependence of RU for the DMPE-containing bilayers. Moreover, there appeared to be a non-linear dependence of RU on concentration between lower and higher concentrations particularly for L-kalata between 40 and 50 μM on the DMPE-containing bilayers. These results suggest that

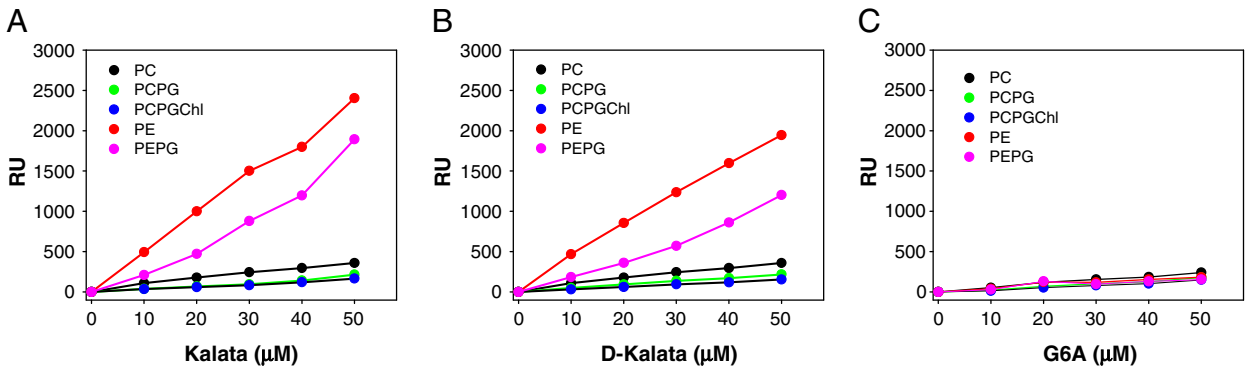

Fig. 4. Plot of RU versus peptide concentration for (A) L-kalata B1, (B) D-kalata B1 and (C) G6A. RU values correspond to RU at the end of the association phase at 200 s. Black = DMPC, Green = DMPC/DMPG, Blue = DMPC/DMPG/cholesterol, Red = DMPE, Pink = DMPE/DMPG.

the DMPE-bound kalata may facilitate a higher amount of kalata binding which leads to higher RU values observed at high kalata concentration. It is also evident from Fig. 4 that the system does not approach equilibrium or saturation.

3.3. Membrane morphology

The interaction of kalata B1 with membranes was also investigated by atomic force microscopy on DMPC and DMPE membrane layers to determine if it caused changes in membrane morphology. Fig. 5A is an image of a large membrane patch of DMPC toward the top left of the image and a smaller patch below it on a flat mica surface. A large open area of mica is on the right. The green bar is the point at which a cross section profile of the lipid layer was taken. Following imaging of the bilayer to ensure the stability of the deposited bilayer material following rinsing with buffer [31], the profile showed the lipid layer to be ~3.5 nm in height. 15 μl of 10 μM of kalata B1 was injected immediately following this image. Fig. 5B corresponds to 12 min after injection. There was a slight change in the shape of the large membrane patch, but was not a significant change. Fig. 5C is an image 32 min after injection. The shape of the patch had changed further with a more angular point where it had previously been more rounded. Fig. 5D corresponds to an image of the surface 64 min after injection of peptide with a higher resolution scan. The edges of the large membrane patch are rougher than previous images. This effect is partially exaggerated due to the higher resolution. Fig. 5E is a scan of the surface 76 min after injection of kalata B1. Material was deposited on the bare mica patch on the right hand side. Fig. 5F corresponds to 87 min after injection and more material had deposited on the mica. The green bar corresponds to a cross section which shows that the deposited material was a few nm in height. Overall, there was no evidence of extensive changes in the DMPC morphology by kalata B1.

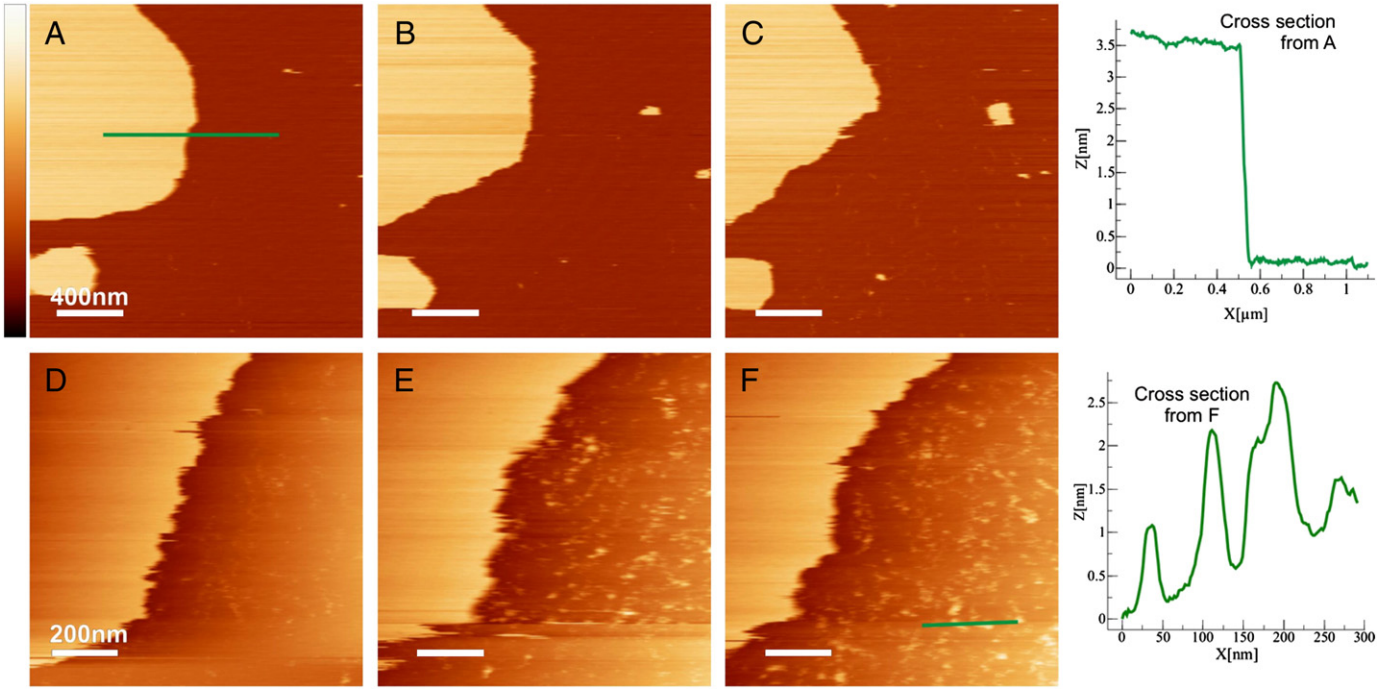

Fig. 5. A series of AFM images of the effect of kalata B1 on DMPC. A) A model bilayer of DMPC that is ~3.5 nm in height as seen by cross section at the top far right from the green bar. 15 μl of 10 m M peptide was then injected immediately after this image. B) 12 min after injection, the shape of the large patch has altered slightly. C) 32 min, the shape of the large patch has changed again D) 64 min after injection, this is a higher resolution image. E) 76 min, material began to deposit on the mica surface on the right hand side of the image. F) 87 min, more material can be seen. Cross section of the green bar shows that the deposited material on the mica was a few nm in height. Scale bar is 400 nm for A–C and 200 nm for D–F. Vertical coloured scale is 8 nm.

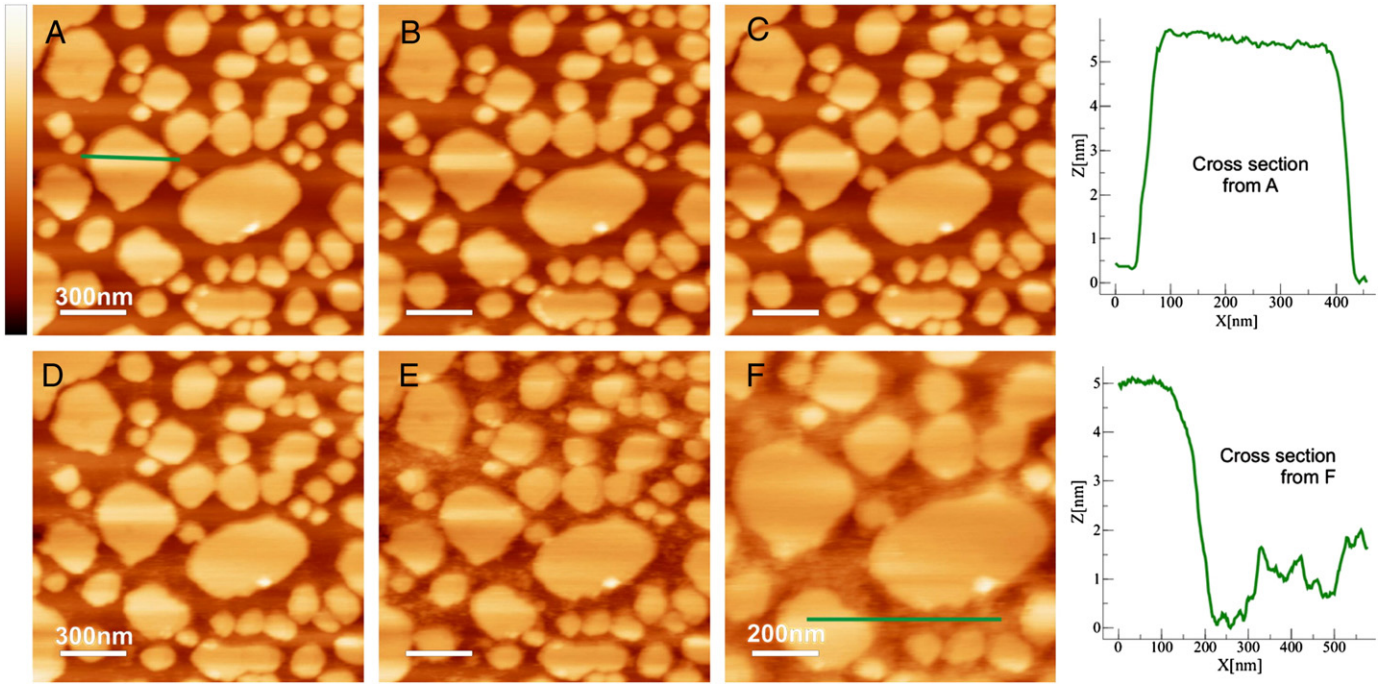

Fig. 6. A series of AFM images of the effect of kalata B1 on DMPE. A) Shows a multitude of DMPE bilayer patches that are ~5.5 nm in height from the cross section (green bar). 15 ml of 10 mM peptide was then injected after this image. B) 12 min after injection, with no visible change. C) 23 min after injection. D) 44 min after injection, a small amount of material was seen deposited between the bilayer patches. E) 578 min, the amount of material has increased. F) 79 min after injection, a higher resolution image. A large amount of material was seen between the patches. A cross section can be seen on the right showing that the deposited material on the mica was a few nm in height. Scale bar is 300 nm for A–E and 200 nm for F. Vertical coloured scale is 13 nm.

Fig. 6A is an image of multiple DMPE membrane patches on a flat mica surface that are ~5.5 nm in height as can be seen by the cross section profile from the green bar. 15 μl of 10 μM kalata B1 was injected immediately after this image. Fig. 6B corresponds to 12 min after injection with no change in morphology observed. Fig. 6C corresponds to 23 min after injection and again no real change in morphology was apparent. Fig. 6D is an image of the surface 44 min after injection of kalata B1. A small amount of material had deposited in between the membrane patches on the mica. Fig. 6E corresponds to 57 min after injection of peptide. A lot more material was observed on the mica areas in between the DMPE patches. Fig. 6F is a higher resolution scan of the surface 79 min after peptide injection. A lot of soft material was observed in between the membrane patches. A cross section (green bar) revealed that the material was a few nm in height. Again there was no evidence of any extensive changes in the DMPE membrane morphology by kalata B1.

4. Discussion

The cyclic backbone and cystine knot have made cyclotides very attractive for molecular scaffold design applications. They are resistant to thermal and chemical breakdown, and therefore have potential as a stable scaffold for antimicrobial peptide design. Kalata B1 has been reported to have antimicrobial activity [14,23] and has previously [31] been shown to interact with and disrupt membranes [15,16], possibly by forming a self-associating multimeric species [18]. The aim of this study was to further explore the membrane binding properties of kalata B1 and two analogues in order to gain further insight into the mechanism of membrane binding and lysis.

The first analogue contained all-D amino acids and although it exhibits lower cytotoxic and nematocidal activity [32] to the native protein, both L- and D-kalata B1 disrupt the membrane of RBCs [22]. This previous study thus demonstrated that a stereo-specific receptor is not crucial for biological activity. The weaker activity of D-kalata B1 also correlated with a lower affinity for phospholipids in model membranes, suggesting that both isoforms act via a similar mechanism that is dependent on membrane interaction [22]. The second analogue has a single substitution of Gly for Ala at the 6th residue which results in a dramatic loss of haemolytic and insecticidal activity [23]. This present study therefore investigated whether these differences in activity are related to a change in membrane binding on different model bilayers by SPR.

Kalata B1 adopted a predominately β-sheet like structure, similar to previous results [20,33], and consistent with the three dimensional structure established from NMR studies, showing that the peptide contains a series of β-turns and loops and a distorted triple-stranded β-sheet [19]. Kalata B1 retained this structure in buffer and in the presence of different mixtures of liposomes, indicating that it is a stable conformation and that the components of the lipid mixtures do not dramatically affect the structure. Other CD studies have also shown that the peptide is very resistant to conformational changes: for example, attempts at thermal (up to 90 °C) and chemical denaturation of kalata B1 revealed little change in the structure [20].

The membrane interaction of kalata B1 showed similar binding to each PC containing mixture (DMPC, DMPC/DMPG (4:1) and DMPC/DMPG/cholesterol (16:4:5)) (Figs. 3 and 4). The binding was moderate on these lipids, with relative binding levels decreasing in the order DMPC > DMPC/DMPG > DMPC/DMPG/cholesterol. However, the interaction with membranes containing DMPE was dramatically enhanced, with kalata B1 showing a 3–10 fold increase in response compared to membrane layers containing DMPC, and is consistent with results obtained previously with palmitolyloleyl-phosphatidylcholine (POPC), palmitolyloleyl-phosphatidylethanolamine (POPE) and palmitolyloleyl-phosphatidylglycerol (POPG) mixtures [34]. The results suggest that kalata B1 is able to bind the DMPE-containing mixtures and also partially penetrate the bilayer, as evident from the slower dissociation and residual binding on these lipid mixtures. DMPE is zwitterionic, as is DMPC, but has a relatively smaller head group which allows a tighter packing of the membrane compared to DMPC (*24*) which in turn leads to a more upright orientation of the head group. This change in head group

orientation has thus allowed kalata B1 to interact more strongly with the membrane surface in both DMPE and DMPE/DMPG mixtures. It is unlikely that the increased binding is due to increased electrostatic interactions as kalata B1 has only one positively charged residue (Arg_{28}) and therefore has a low propensity to interact via strong electrostatic interactions. Moreover, the addition of anionic DMPG to the mixture resulted in a small decrease in the amount of peptide bound. The Arg_{28} residue has been previously shown to be critical for antimicrobial activity [14], and might be essential for the initial stages of membrane binding through electrostatic interactions. Other macrocyclic peptides such as circulin B and cyclopsychotride have a cluster of three cationic residues and are active against gram negative bacteria such as *Escherichia coli* whereas kalata B1, which contains a single positive charge, is inactive, suggesting that cationic residues are important for the cytolytic activity (*14*). This is also consistent with a recent study on the membrane binding effects of cycloviolacin O2, a cyclotide that has more positive charges (+3) than kalata B1 and has higher affinity for anionic lipids [35].

With such a dramatic difference in membrane binding of kalata B1 on DMPC- and DMPE-containing lipids, it might be expected that there would be a substantial difference in the effect of kalata B1 on the morphology of each lipid bilayer. However, this was not the case, with kalata B1 interacting in a similar way on both lipid mixtures as imaged by AFM, suggesting that the mechanism of action of this peptide is not likely to be mediated by general membrane disruption or a carpet-like mechanism. This result is consistent with a recent report that used electrophysiology to demonstrate that kalata B1 forms pores upon binding to a range of phospholipid bilayers [17]. The pores were reported to measure 41–47 Å in diameter, which is at the resolution limits of the AFM measurements.

The all D-kalata B1 peptide interacted in a similar way to the L-peptide with a similar association, binding response and dissociation on the lipids containing DMPC (Fig. 3). It also had the lowest binding interaction with DMPC/DMPG/cholesterol, which could once again be due to the membrane stabilizing effect of cholesterol inhibiting binding. Interestingly, D-kalata B1 also showed the same high binding selectivity for DMPE lipids (but with slightly lower levels). Although the phospholipid mixtures are model membrane systems, a close correlation of haemolytic effects with membrane affinities for L and D-kalata B1 was previously observed [22]. The same study also demonstrated that biological activity depends on peptide oligomerization at the membrane surface, which determines affinity for membranes by modulating the association/dissociation equilibrium [22]. Overall, the results of the present study confirm that the binding interaction and the binding selectivity for DMPE membranes is not a stereospecific interaction. Although it has been demonstrated that PE phospholipids containing unsaturated acyl chains preferentially adopt a hexagonal phase structure [36,37], fully saturated PE phospholipids are known to adopt a lamellar structure [38]. Since we have utilised DMPE in this study, it is most likely that the model membranes in our study exist as a bilayer structure. Moreover, the preparation of the DMPE liposomes yielded a clear solution upon lipid rehydration and vortexing consistent with the formation of lamellar structure rather than a hexagonal phase, which yields a cloudy solution. The resultant DMPE lipid bilayers imaged in the AFM experiments also confirm the presence of bilayers of 5 nm in height (Fig. 6).

The G6A analogue also showed similar membrane binding to L-kalata B1 and D-kalata B1 on the DMPC lipids, with the same relatively weak interaction. However, in contrast to L-kalata B1 and D-kalata B1, the G6A analogue did not show any substantial binding selectivity for DMPE. This is a significant result and suggests that the composition of the surface topography in this region of kalata B1 plays an important role in the membrane interaction. A previous NMR study showed that the conformation of G6A was almost identical to kalata B1, confirming that this substitution does not influence the secondary structure [23]. However, while the overall structure of this analogue is nearly identical to kalata B1, the biological activity is vastly different [23], suggesting that Gly_6 plays a more critical role in the biological activity via an effect on the surface topography rather than via an overall effect on the structure of the peptide. A similar conclusion has been reached with other disulfide rich peptides such as the α-conotoxins that have sequence diversity while still maintaining a common three dimensional structure [39,40]. This suggestion is further supported by the observation that linear versions of kalata B1 that have essentially the same structure as the cyclic peptide but a different surface topography are inactive [41].

Previous studies have suggested that a cluster of hydrophobic residues that form a solvent exposed patch on kalata B1 mediates interaction with the membrane [19]. A closer examination of the localization of the hydrophobic residues within kalata B1 as shown in Fig. 7A, reveals that Gly_6 is not located in this hydrophobic 'patch', but lies adjacent to it [23]. Recent spin labelled NMR studies have also demonstrated that this surface exposed hydrophobic patch forms the membrane binding face of kalata B1 with DPC micelles [42] which includes Gly_6 at the edge of this region as seen in Fig. 7B. Studies using analytical ultracentrifugation have also shown that kalata B1 forms tetramers in sodium phosphate buffer [18]. Moreover, the recent demonstration that kalata B1 forms pores [17] suggests that specific oligomerization along with membrane binding is vital for the activity of kalata B1. Regions that have been shown to be critical to activity have been found to lie orthogonal to the hydrophobic regions of kalata B1 [23]. This would be consistent with a self association model in which four molecules come together, with the activity-influencing hydrophilic surfaces facing inward and the hydrophobic surfaces oriented on the face of the tetramer [23] as shown in Fig. 7C. It is possible that the Gly_6 residue lies within a region that would affect the propensity for self association and mutations of this reside may hinder the ability of kalata B1 to self associate and thereby reduce membrane binding.

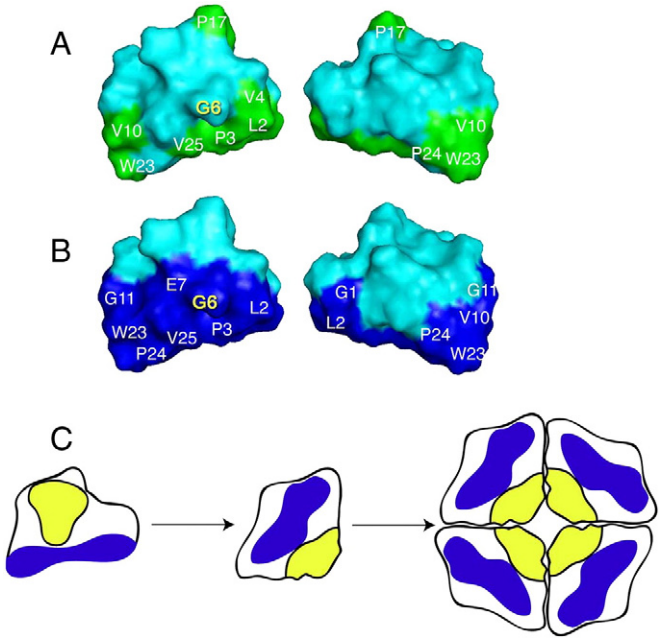

Fig. 7. A) Localization of the hydrophobic residues within kalata B1 that form a hydrophobic patch shown in green. B) Membrane penetrating residues as measured by NMR [42] shown in dark blue. Images on the right are 180° relative to those on the left. C) Schematic representation of a possible tetramer model of kalata B1. The blue regions represent the hydrophobic surface patch known to be associated with membrane binding, and the yellow regions represent the hydrophilic face that is correlated with bioactivity.
Modified from [23].

5. Conclusion

L-Kalata B1 and D-kalata B1 show strong selectivity towards DMPE-containing lipids compared to DMPC-containing membranes but do not cause any significant change in membrane morphology, suggesting that the all-D analogue exerts its action via the same mechanism as the all-L peptide. By comparison, the strong selectivity for DMPE was totally eliminated in the G6A analogue, indicating that the Gly_6 residue has a significant role in the selective membrane interaction. Overall, this study demonstrates that a single amino acid substitution, which renders kalata B1 inactive, has also significantly altered the membrane binding properties and might represent a critical step in the cytolytic mechanism of kalata B1. This finding thus has implications in the design of novel selective antimicrobial peptides which are non-toxic to the host organism.

References

[1] D.J. Craik, N.L. Daly, T. Bond, C. Waine, Plant cyclotides: a unique family of cyclic and knotted proteins that defines the cyclic cystine knot structural motif, J. Mol. Biol. 294 (1999) 1327–1336.
[2] D.J. Craik, N.L. Daly, C. Waine, The cystine knot motif in toxins and implications for drug design, Toxicon 39 (2001) 43–60.
[3] C. Jennings, J. West, C. Waine, D. Craik, M. Anderson, Biosynthesis and insecticidal properties of plant cyclotides: the cyclic knotted proteins from *Oldenlandia affinis*, Proc. Natl. Acad. Sci. U.S.A. 98 (2001) 10614–10619.
[4] D.J. Craik, M.A. Anderson, D.G. Barry, R.J. Clark, N.L. Daly, C.V. Jennings, J. Mulvenna, Discovery and structures of the cyclotides: novel macrocyclic peptides from plants, Lett. Pept. Sci. 8 (2002) 119–128.
[5] L. Gran, Oxytocic principles of *Oldenlandia affinis*, Lloydia 36 (1973) 174–178.
[6] L. Gran, F. Sandberg, K. Sletten, Oldenlandia affinis (R&S) DC, A plant containing uteroactive peptides used in African traditional medicine, J. Ethnopharmacol. 70 (2000) 197–203.
[7] K.R. Gustafson, R.C. Sowder, I.L.E. Henderson, I.C. Parsons, Y. Kashman, J.H. Cardellina, I.J.B. McMahon, R.W. Buckheit, J.L.K. Pannell, M.R. Boyd, Circulins A and B. Novel human immunodeficiency virus (HIV)-inhibitory macrocyclic peptides from the tropical tree Chassalia parvifolia. J. Am. Chem. Soc. 116 (1994) 9337–9338.
[8] K.M. Witherup, M.J. Bogusky, P.S. Anderson, H. Ramjit, R.W. Ransom, T. Wood, M. Sardana, Cyclopsychotride A, a biologically active, 31-residue cyclic peptide isolated from *Psychotria longipes*, J. Nat. Prod. 57 (1994) 1619–1625.
[9] T. Schopke, M.I. Hasan Agha, R. Kraft, A. Otto, K. Hiller, Compounds with hemolytic activity from *Viola tricolor* L. and *Viola arvensis murray*, Sci. Pharm. 61 (1993) 145–153.
[10] A.M. Broussalis, U. Göransson, J.D. Coussio, G. Ferraro, V. Martino, P. Claeson, First cyclotide from *Hybanthus* (Violaceae), Phytochemistry 58 (2001) 47–51.
[11] C.V. Jennings, K.J. Rosengren, N.L. Daly, M. Plan, J. Stevens, M.J. Scanlon, C. Waine, D.G. Norman, M.A. Anderson, D.J. Craik, Isolation, solution structure, and insecticidal activity of kalata B2, a circular protein with a twist: do Mobius strips exist in nature? Biochemistry 44 (2005) 851–860.
[12] P. Lindholm, U. Goransson, S. Johansson, P. Claeson, J. Gullbo, R. Larsson, L. Bohlin, A. Backlund, Cyclotides: a novel type of cytotoxic agents, Mol. Cancer Ther. 1 (2002) 365–369.
[13] H.R. Bokesch, L.K. Pannell, P.K. Cochran, R.C. Sowder 2nd, T.C. McKee, M.R. Boyd, A novel anti-HIV macrocyclic peptide from *Palicourea condensata*, J. Nat. Prod. 64 (2001) 249–250.
[14] J.P. Tam, Y.A. Lu, J.L. Yang, K.W. Chiu, An unusual structural motif of antimicrobial peptides containing end-to-end macrocycle and cystine-knot disulfides, Proc. Natl. Acad. Sci. U.S.A. 96 (1999) 8913–8918.
[15] H. Kamimori, K. Hall, D.J. Craik, M.I. Aguilar, Studies on the membrane interactions of the cyclotides kalata B1 and kalata B6 on model membrane systems by surface plasmon resonance, Anal. Biochem. 337 (2005) 149–153.
[16] E. Svangard, R. Burman, S. Gunasekera, H. Lovborg, J. Gullbo, U. Goransson, Mechanism of action of cytotoxic cyclotides: cycloviolacin O2 disrupts lipid membranes, J. Nat. Prod. 70 (2007) 643–647.
[17] Y.H. Huang, M.L. Colgrave, N.L. Daly, A. Keleshian, B. Martinac, D.J. Craik, The biological activity of the prototypic cyclotide kalata b1 is modulated by the formation of multimeric pores, J. Biol. Chem. 284 (2009) 20699–20707.
[18] A. Nourse, M. Trabi, N.L. Daly, D.J. Craik, A comparison of the self-association behavior of the plant cyclotides kalata B1 and kalata B2 via analytical ultracentrifugation, J. Biol. Chem. 279 (2004) 562–570.
[19] O. Saether, D.J. Craik, I.D. Campbell, K. Sletten, J. Juul, D.G. Norman, Elucidation of the primary and three-dimensional structure of the uterotonic polypeptide kalata B1, Biochemistry 34 (1995) 4147–4158.
[20] M.L. Colgrave, D.J. Craik, Thermal, chemical, and enzymatic stability of the cyclotide kalata B1: the importance of the cyclic cystine knot, Biochemistry 43 (2004) 5965–5975.
[21] J.F. Hernandez, J. Gagnon, L. Chiche, T.M. Nguyen, J.P. Andrieu, A. Heitz, T. Trinh Hong, T.T. Pham, D. Le Nguyen, Squash trypsin inhibitors from *Momordica cochinchinensis* exhibit an atypical macrocyclic structure, Biochemistry 39 (2000) 5722–5730.
[22] L. Sando, S.T. Henriques, F. Foley, S.M. Simonsen, N.L. Daly, K. Hall, N., K.R. Gustafson, M.I. Aguilar, D.J. Craik, A synthetic mirror image of kalata B1 reveals that cyclotide activity is independent of a protein receptor, ChemBioChem. 12 (2011) 2456–2462.
[23] S.M. Simonsen, L. Sando, K.J. Rosengren, C.K. Wang, M.L. Colgrave, N.L. Daly, D.J. Craik, Alanine scanning mutagenesis of the prototypic cyclotide reveals a cluster of residues essential for bioactivity, J. Biol. Chem. 283 (2008) 9805–9813.
[24] T.H. Lee, H. Mozsolits, M.I. Aguilar, Measurement of the affinity of melittin for zwitterionic and anionic membranes using immobilized lipid biosensors, J. Pept. Res. 58 (2001) 464–476.
[25] H. Mozsolits, M.I. Aguilar, Surface plasmon resonance spectroscopy: an emerging tool for the study of peptide–membrane interactions, Biopolymers 66 (2002) 3–18.
[26] H. Mozsolits, H.J. Wirth, J. Werkmeister, M.I. Aguilar, Analysis of antimicrobial peptide interactions with hybrid bilayer membrane systems using surface plasmon resonance, Biochim. Biophys. Acta 1512 (2001) 64–76.
[27] I. Horcas, R. Fernandez, J.M. Gomez-Rodriguez, J. Colchero, J. Gomez-Herrero, A.M. Baro, WSXM: a software for scanning probe microscopy and a tool for nanotechnology, Rev. Sci. Instrum. 78 (2007) 013705.
[28] K. Hall, M.I. Aguilar, Membrane interactions of antimicrobial beta-peptides: the role of amphipathicity versus secondary structure induction, Biopolymers 92 (2009) 554–564.
[29] K. Hall, T.H. Lee, M.I. Aguilar, The role of electrostatic interactions in the membrane binding of melittin, J. Mol. Recognit. 24 (2011) 108–118.
[30] K. Hall, H. Mozsolits, M. Aguilar, Surface plasmon resonance analysis of antimicrobial peptide–membrane interactions: affinity & mechanism of action, Lett. Pept. Sci. 10 (2003) 475–485.
[31] A. Mechler, S. Praporski, S. Piantavigna, S.M. Heaton, K.N. Hall, M.I. Aguilar, L.L. Martin, Structure and homogeneity of pseudo-physiological phospholipid bilayers and their deposition characteristics on carboxylic acid terminated self-assembled monolayers, Biomaterials 30 (2009) 682–689.
[32] M.L. Colgrave, A.C. Kotze, Y.H. Huang, J. O'Grady, S.M. Simonsen, D.J. Craik, Cyclotides: natural, circular plant peptides that possess significant activity against gastrointestinal nematode parasites of sheep, Biochemistry 47 (2008) 5581–5589.
[33] N.L. Daly, S. Love, P.F. Alewood, D.J. Craik, Chemical synthesis and folding pathways of large cyclic polypeptides: studies of the cystine knot polypeptide kalata B1, Biochemistry 38 (1999) 10606–10614.
[34] S.T. Henriques, Y.H. Huang, K.J. Rosengren, H.G. Franquelim, F.A. Carvalho, A. Johnson, S. Sonza, G. Tachedjian, M.A. Castanho, N.L. Daly, D.J. Craik, Decoding the membrane activity of the cyclotide kalata B1: the importance of phosphatidylethanolamine phospholipids and lipid organization on hemolytic and anti-HIV activities, J. Biol. Chem. 286 (2011) 24231–24241.
[35] R. Burman, A.A. Stromstedt, M. Malmsten, U. Goransson, Cyclotide-membrane interactions: defining factors of membrane binding, depletion and disruption, Biochim. Biophys. Acta 1808 (2011) 2665–2673.
[36] R.N. Lewis, D.A. Mannock, R.N. McElhaney, D.C. Turner, S.M. Gruner, Effect of fatty acyl chain length and structure on the lamellar gel to liquid-crystalline and lamellar to reversed hexagonal phase transitions of aqueous phosphatidylethanolamine dispersions, Biochemistry 28 (1989) 541–548.
[37] J.M. Seddon, Structure of the inverted hexagonal (HII) phase, and non-lamellar phase transitions of lipids, Biochim. Biophys. Acta 1031 (1990) 1–69.
[38] A.M. Bouchet, M.A. Frias, F. Lairion, F. Martini, H. Almaleck, G. Gordillo, E.A. Disalvo, Structural and dynamical surface properties of phosphatidylethanolamine containing membranes, Biochim. Biophys. Acta 1788 (2009) 918–925.
[39] S.H. Hu, J. Gehrmann, P.F. Alewood, D.J. Craik, J.L. Martin, Crystal structure at 1.1 A resolution of alpha-conotoxin PnIB: comparison with alpha-conotoxins PnIA and GI, Biochemistry 36 (1997) 11323–11330.
[40] A. Nicke, M.L. Loughnan, E.L. Millard, P.F. Alewood, D.J. Adams, N.L. Daly, D.J. Craik, R.J. Lewis, Isolation, structure, and activity of GID, a novel alpha 4/7-conotoxin with an extended N-terminal sequence, J. Biol. Chem. 278 (2003) 3137–3144.
[41] D.G. Barry, N.L. Daly, R.J. Clark, L. Sando, D.J. Craik, Linearization of a naturally occurring circular protein maintains structure but eliminates hemolytic activity, Biochemistry 42 (2003) 6688–6695.
[42] Z.O. Shenkarev, K.D. Nadezhdin, V.A. Sobol, A.G. Sobol, L. Skjeldal, A.S. Arseniev, Conformation and mode of membrane interaction in cyclotides. Spatial structure of kalata B1 bound to a dodecylphosphocholine micelle, FEBS J. 273 (2006) 2658–2672.